Lecture 20, October 28, 2010 (Key Points)

Introduction

The objective of this lecture, and the next few lectures, is to explain steps that are required to gain a physical understanding of the observed power laws in peak flows for rainfall-runoff (RO-RF) events in the Goodwin Creek Experimental Watershed (GCEW), MS that was introduced in Lecture 10. They build on the physical concepts covered in Lectures 14-19. A diagnostic framework is necessary to physically understanding how power laws in peak flows arise and to develop reliable models for flood prediction in ungauged basins. The diagnostic framework is not specific to GCEW covered here, and can be applied to understanding space-time patterns in any basin. It consists of five steps (Furey and Gupta 2007):

1. Identify and quantify a recurring space-time pattern in data.
2. Use datasets that complement the data in step 1 to show, qualitatively, how certain conditions and processes influence the pattern.
3. Develop theoretical expressions and/or run simulations to describe how the pattern depends on the conditions and physical processes examined in step 2.
4. Test the results of step 3 against those in step 2.
5. Assess the test results from step 4 and repeat, if necessary, steps 2–5.

A model requiring calibration that is a common practice in engineering hydrology should not be used to pursue step 3. Therefore, the word ‘simulation’ is used here. Step 5 is an assessment of how well the physical origin of the recurring pattern has been explained and provides a basis for introducing more complexity, if necessary, into steps 2 and 3.

Ogden and Dawdy (2003) took step 1 in their investigation of peak stream flows in GCEW. The recurring space-time pattern they identified is a power law that is present from event-to-event. They used a least-squares linear regression to quantify the power law parameters. Furey and Gupta (2005) took step 2. Guided by past research results and using a combination of streamflow and rainfall data, they showed, qualitatively, how the depth and duration of estimated excess rainfall influences peak discharge power laws in GCEW. Fury and Gupta (2007) investigated steps 3–5. Above results will be briefly explained.

20.1 Power laws in floods for rainfall-runoff events in GCEW

It is difficult to directly use annual flood quantile data to understand the physical basis of power laws, or *scaling statistics* (Lecture 4). The difficulty arises because quantiles of the same return period can be associated with floods from different RF-RO events. This issue led to analyzing the scaling statistics of peak flows for a single RF-RO event at multiple gauging stations throughout a river basin. Such data sets are not commonly available. One such basin with such data sets is GCEW. Ogden and Dawdy (2003) observed the presence of power laws in peak flows for a large number of RF-RO events, and in annual flood quantiles in GCEW. Fig. 20.1 shows the power laws and corresponding slopes for four RF-RO events. It was the first paper in the hydrologic literature to conduct an event based spatial scaling analysis of peak flows.

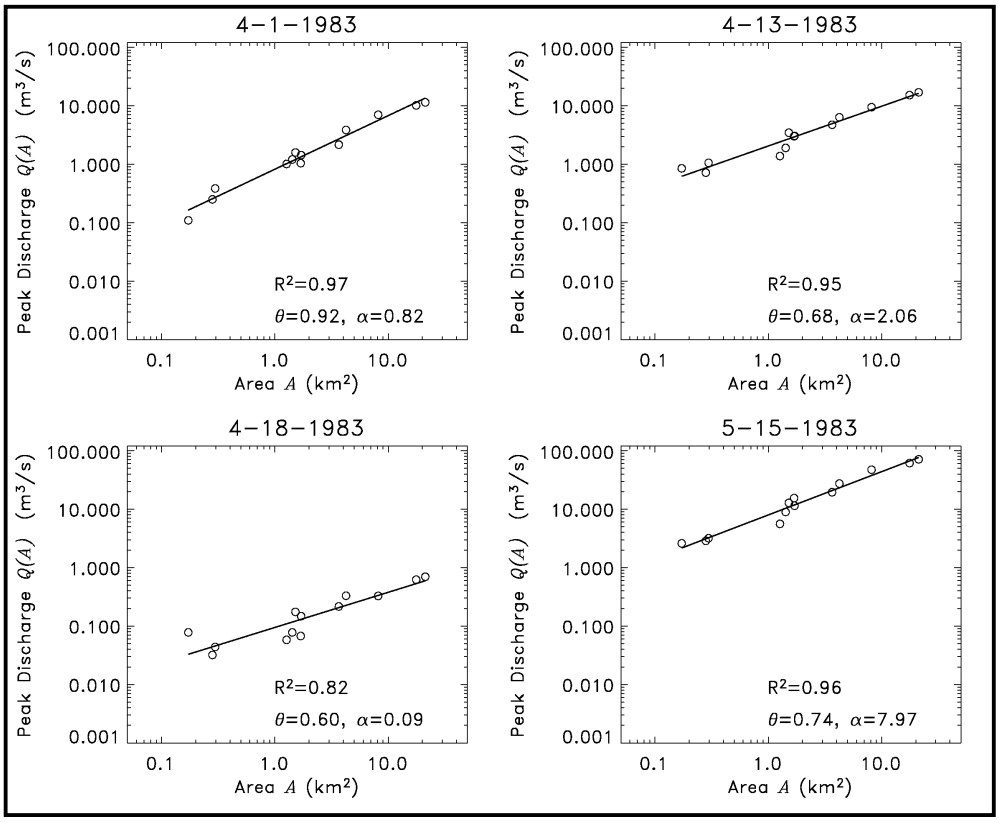

Fig. 20.1 Power laws in spatial variability in peak flows for different rainfall-runoff events with different slopes on Goodwin Creek, MS (Ogden and Dawdy, 2003).

20.2 Test of GIUH prediction against scaling in peak flows in GCEW

This section explains how predictions of the width-function GIUH for peak flows can be tested with data in Fig. 20.1. Recall that a GIUH arises under two assumptions: (i) runoff is applied spatially uniformly and instantaneously on a network, and (ii) water flows with a constant flow velocity through the network without a change in channel storage. Under GIUH theory, the hydrograph maps exactly onto a width function. Each channel junction of a river network is an outlet for the basin upstream of it, and therefore has its own width function as explained in Lecture 19 (Section 19.3). Theoretically, under the GIUH, scaling properties of the width function should be expressed in the hydrograph. We computed the maxima of the width functions (W_p) above the ends of all Strahler-ordered streams in GCEW and above the stream gauging stations responsible for the data in Fig. 20.1. The plot in Fig. 20.2 shows a scaling relation between W_p and drainage area A, which is a consequence of self-similarity in channel network geometry (Veitzer and Gupta 2001).

Slope in the scaling relation in Fig. 20.2 is 0.43, a prediction of the GIUH theory for scaling in peak flows. However, the slopes of the scaling relation in observed peak flows in Fig. 20.1 (left panel) range from 0.6-0.9. The discrepancies between observations in

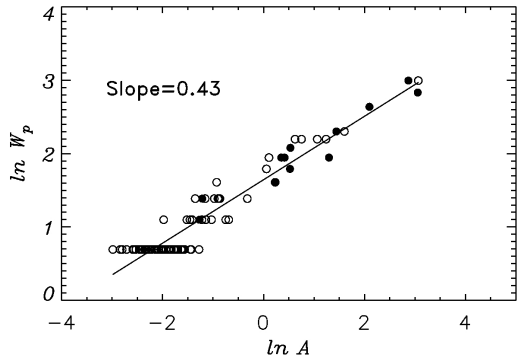

Figure 20.2. The logarithm of the peak of the width function *ln* W_p versus the logarithm of drainage area *ln A* for GCEW. Only basins with W_p >1 are plotted. Filled circles denote stream gauge locations. Empty circles denote the ends of complete Strahler-order streams.

Fig. 20.1, and between the GIUH theory and observations in Fig. 20.2, demonstrate that, to predict scaling in peak flows, more information is needed about the physical processes occurring in a RF-RO event than assumed in the GIUH theory, e.g. space-time variability in rainfall and in runoff generation and transport.

Scaling relations represent dominant signature of a few critical relationships in a complex non-linear system. Our objective is to understand the key physical relationships that are needed to predict the slopes and the intercepts of the scaling relations. We will see how *scaling provides a basis to develop a diagnostic framework to understand multi-scale complexity of hydrologic processes in a river basin.*

20.3 Predicting Scaling Slope and Intercept from Physical Processes: An Example

Furey and Gupta (2005) investigated how and why the parameters in peak discharge power laws change from one event to another. They examined peak discharges from 148 events in GCEW, and found that the change is directly related to temporal variability in the time series of excess rainfall. This is an important finding, because it suggests that power laws in peak flows are linked with physical processes on channel networks that transform rainfall to runoff.

Building on this finding, Furey and Gupta (2007) developed a diagnostic framework to predict slopes and intercepts of peak flow scaling functions. The approach consists of representing discharge from any sub basin of drainage area A at time *t*>0 during a single RF-RO event as,

$$Q_A(t) = \int_0^t R(s) W_A(v(t-s)/l)\,ds; \quad t < T \tag{20.1}$$

Here, the integral is a convolution in time. $\{R(s); s \geq 0\}$ is a stochastic process representing the excess-rainfall that enters a channel from adjacent hillslope, and $W_A(v(t-s))/l$ is a stochastic process representing the basin's response function during an event (*We will make an excursion and define the concept of a stochastic process given at the end of this lecture). Note that the basin's response function is not the same as the width function GIUH, because the assumption that $dS/dt = 0$ in Eq. (19.1) is not used here. Here, *v* represents an effective runoff velocity for the basin that is uniform in space and constant in time, *l* is the mean distance that water travels through a network link and *T* is the duration of a rainfall–runoff event. An event starts when excess-rainfall generation begins and ends when streamflow response finishes. Runoff velocity *v* is

assumed to be constant in time and space.

Furey and Gupta (2007) calculated mean discharge, $E[Q_A(t)|D_1, D_{2,A}]$ conditioned on excess rainfall duration, D_1 and the duration of the basin-response function, $D_{2,A}$. Taking the conditional expectation in Eq. 20.1 gives a space-time representation of conditional mean discharge (Furey and Gupta, 2007, p. 2393) as,

$$E[Q_A(t)|D_1, D_{2,A}] = \int_0^t E[R(s)|D_1] E[W_A(v(t-s)/l)|D_{2,A}] ds; \quad t < T \tag{20.2}$$

It involves two conditional mean functions, $E[R(s)|D_1]$ representing mean excess rainfall given duration, and $E[W(v(t-s)/l)|D_{2,A}]$ representing mean basin response function given its duration. Eq. (20.2) represents a stochastic generalization of GIUH in a convolution equation (Lecture 16).

20.3.1 mean excess rainfall given duration

$E[R(s)|D_1]$ was calculated by using spatially averaged time series for each of 148 RF-RO events in the basin, and applying an infiltration threshold "loss rate independent of rainfall intensity" (Brutsaert, 2005, p. 345) It is also called the Phi-Index Method in the engineering hydrology literature. It is a water balance method applied to spatially averaged rainfall intensity and streamflow hydrograph at the outlet of a basin.

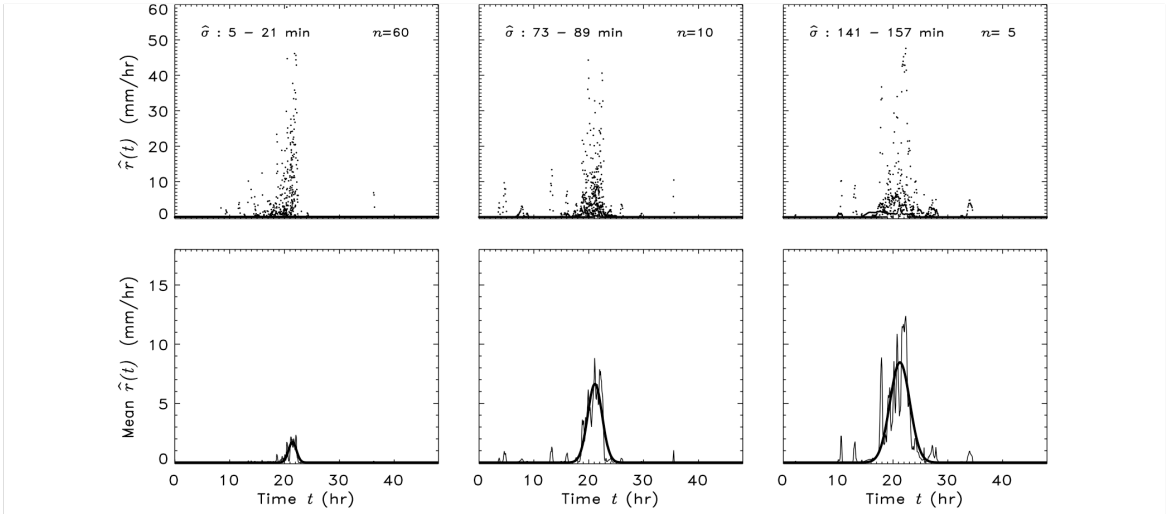

Fig. 2. Top plots show values of $\hat{r}(t)$ versus t conditioned on a narrow range of values for the estimated duration of excess-rainfall, $\hat{\sigma}$. In each plot, there are n time series of $\hat{r}(t)$. For each time series, the corresponding peak streamflow at the outlet of GCEW occurs at $t = 24$; thus, time is centered on ±24 h from the time of peak streamflow at the outlet. Points for each time series are unconnected to preserve graphical clarity. Bottom plots show corresponding mean values of $\hat{r}(t)$ versus t (thin line) and a fitted Gaussian density function (thick line).

Figure 20.3 Mean excess rainfall time series given duration

20.3.2 mean basin response function given duration

Streamflow hydrographs were simulated throughout GCEW by solving a coupled set of network based mass and momentum conservation Eqs. (19.1) and (19.2). CUENCAS solves the coupled equations numerically and simulates hydrographs at all channel links in a network. Simulations were limited to a few basic physical processes and conditions in order to gain an understanding of their interaction and influence. The

topography of GCEW was represented by a DEM of 30 m resolution, which Mantilla and Gupta [15] found to be the lowest resolution that can accurately characterize the network structure of a basin. The river network was extracted from the DEM using CUENCAS and it compared well with Blue Line maps of the basin.

An 'instantaneous' pulse of excess rainfall with a depth of 0.001 m (1 mm) was used to force a simulation. To represent this pulse, each hillslope in GCEW was covered uniformly with water having a depth of 0.001 m and then the basin was allowed to drain. A linear storage–discharge relationship with flow velocity v_h was used to characterize runoff from a hillslope. Likewise, a linear storage–discharge relationship with flow velocity v_l was used to characterize runoff from a link. Hillslope and link dynamics included storage attenuation, and simulated streamflow was sampled at each outlet of the 552 links that comprise the DEM-extracted river network. Under the conditions described above, a simulated hydrograph for a given subbasin in GCEW is a GIUH. Therefore, a simulation produced a family of 552 GIUH's characterizing the sampled subbasins and outlet of GCEW. This family of GIUH's was viewed as a family of response functions, with each response function determined by flow dynamics and network structure. Fig. 3 shows the results of our conditional analysis on simulations where v_h = 0.1 m/s and v_l = 1 m/s.

To make Fig. 3, we first defined a range of areas A and then a range of basin-response durations on which to condition our analysis. We evaluated the duration for each subbasin using a surrogate measure defined as $\tau = q_T(A)/Q(A)$ where $q_T(A)$ = 0.001A is the total discharge volume (m^3) and $Q(A)$ is the simulated discharge peak (m^3/s). The three plots at the top of Fig. 3 show discharge versus time conditioned on a range of A and τ values. The third plot includes the response function for the outlet of GCEW. Plots at the bottom show the time series of mean discharge calculated from each plot at the top, and a corresponding fitted Gaussian density function. Qualitatively,

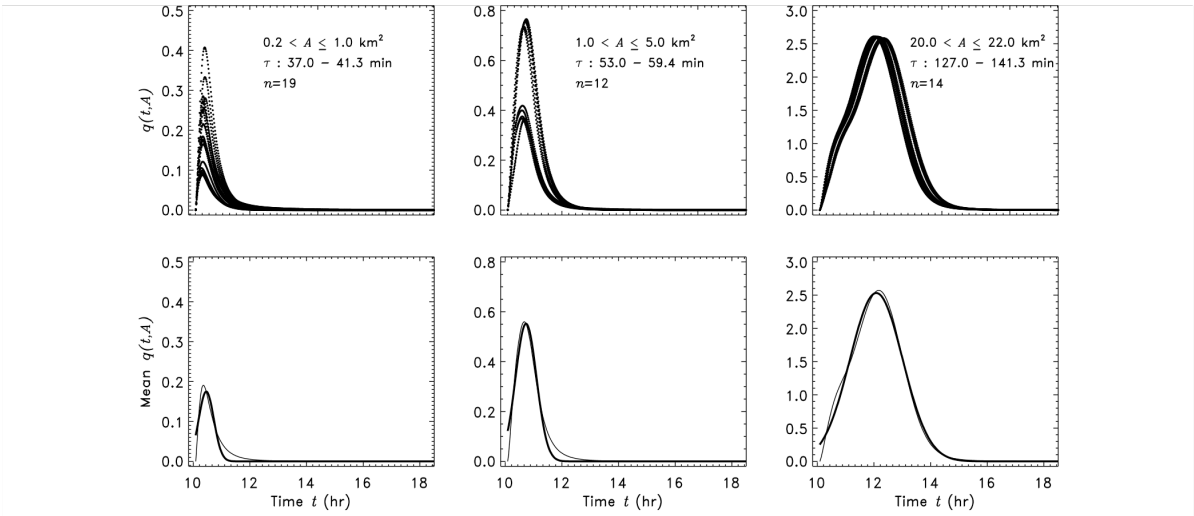

Fig. 3. Simulation results where $v_h = 0.1$ and $v_l = 1.0$ m/s. The first three plots (top) show values of simulated discharge $q(t, A)$ versus t conditioned on a narrow range of values for both A and the estimated duration of the simulated streamflow response, τ. In log space, the size of the range for A is the same for the first two plots. The third plot (top) includes $q(t, A)$ versus t at the outlet of GCEW. The number of hydrographs per plot is indicated by n. Bottom plots show corresponding mean values of $q(t, A)$ versus t (thin line) and a fitted Gaussian density function (thick line).

Figure 20.4 Mean basin response function time series given duration

a Gaussian density captures the mean time series pattern for each group. This

result is also found for other groups of A and τ. This exercise illustrates that a Gaussian density function is a reasonable first-order approximation for the shape of the conditional mean basin-response function when v_h= 0.1 m/s and v_l = 1 m/s. Simulations using other values for v_h and v_l lead to the same conclusion.

Next we will examine how the response function in GCEW changes with respect to drainage area. Each value of τ obtained from a simulation was plotted against *A* in log–log space. τ can be taken as a surrogate for the longest channel length under constant velocity. Hack's law suggests a power-law relation between τ and *A* ….(to be continued in Lecture 21).

(*) **Appendix on a Stochastic Process (Background material)**

The term *stochastic process* (SP) refers to that branch of probability theory, which deals with evolution in time or space, or in space and time. The evolution is described by a sequence or more generally a collection of random variables indexed by a parameter, called an *index parameter*. The index parameter represents time in many applications. It can be either discrete or continuous, and this leads to constructing discrete or continuous parameter stochastic processes. If the index parameter is multidimensional, for example space-time, then a stochastic process is called a *random field.*

Definition 7.1

Given an index set I, a stochastic process indexed by I is a collection of random variables $\{X_\lambda : \lambda \in I\}$ on a probability space $\{\Omega, \Im, P\}$ taking values in a set S. The set S is called the state space.

For a stochastic process, the values of the random variables corresponding to the occurrence of a sample point $\omega \in \Omega$ constitute a *sample realization* of the process. In the case of a continuous parameter stochastic process with index set $I = (0, \infty)$ and state space $\mathbf{R} = (-\infty, \infty)$, the sample realizations are functions $t \to X_t(\omega) \in S,\ \omega \in \Omega$. Sample realizations of a stochastic process are also referred to as *sample paths*. Discrete-parameter stochastic processes are indexed by the set of integers. Continuous-parameter stochastic processes are indexed by an interval, for example, in our case of excess rainfall intensity, $\{R(s); s \geq 0\}$. Random fields are indexed by multi-dimensional parameters, e.g., space-time. For example, in statistical analyses of annual floods in a region, called *regional flood frequency analyses*, annual peak flows $Q(A): A > 0$ can be viewed as a SP over subbasins A with drainage areas $|A|$ within a basin or a region D, such that $A \subset D$. By contrast, a geometric variable on a channel network, $X_\omega : \omega = 1, 2, \ldots$, represents a discrete-parameter SP indexed by the Strahler order ω.

A SP $X(t, \omega);\ t \in I, \omega \in \Omega$ can be thought of as a function of two variables t, ω. For a fixed $t = t^*$, $X(\omega)$ is only a function of ω and therefore is a random variable. For a fixed ω, $X(t)$ is a function of time, and is called a "sample path" or a "sample realization" of a SP. It is a standard convention to suppress ω and simply write $\{X(t); t \in I\}$ for a SP as in Eq. (20.1).

The probabilistic specification of a SP is often prescribed by events that depend on the values of the SP at finitely many time points, $X(t_1), X(t_2), \ldots, X(t_n)$. They are called *finite-dimensional events*. For example, $X(t_1) < x_1, X(t_2) < x_2, \ldots, X(t_n) < x_n$ is a finite dimensional event. The step involved in the construction of a SP on a suitable probability space from knowing the probabilities of all finite-dimensional events is a technical mathematical issue that we will not go into. Prescribing probabilities of events that depend only on finitely many time points often specifies stochastic descriptions of physical phenomena. In many applications, the probabilities of more complex events, e.g., the *infinite-dimensional events,* are calculated in terms of the probabilities of finite-dimensional events by passage to a limit.

References:

Brutsaert, W. *Hydrology: An introduction*, Cambridge, 2005.

Furey, P. R., and V. K. Gupta, Effects of excess rainfall on the temporal variability of observed peak discharge power laws, *Advances in Water Resources* 28, 1240–1253, 2005.

Furey, P. R., and V. K. Gupta, Diagnosing peak-discharge power laws observed in rainfall-runoff events in Goodwin Creek experimental watershed, *Advances in Water Resources*, 30, 2387-2399, 2007.

Ogden, F. L. and D. R. Dawdy, Peak discharge scaling in a small Hortonian watershed, *Journal of Hydrologic Engineering*, 8(2), 64-73, 2003.

Veitzer, S., and V. K. Gupta, Statistical self-similarity of width function maxima with implications to floods, *Advances in Water Resources*, 24, 955–965, 2001.